5-Aminoimidazole-4-Carboxamide Ribonucleoside (AICAR) Inhibits Insulin-Stimulated Glucose Transport in 3T3-L1 Adipocytes

Ian P. Salt, John M. C. Connell, and Gwyn W. Gould

Incubation of skeletal muscle with 5-aminoimidazole-4-carboxamide ribonucleoside (AICAR), a compound that activates 5′-AMP-activated protein kinase (AMPK), has been demonstrated to stimulate glucose transport and GLUT4 translocation to the plasma membrane. In this study, we characterized the AMPK cascade in 3T3-L1 adipocytes and the response of glucose transport to incubation with AICAR. Both isoforms of the catalytic α-subunit of AMPK are expressed in 3T3-L1 adipocytes, in which AICAR stimulated AMPK activity in a time- and dose-dependent fashion. AICAR stimulated 2-deoxy-D-glucose transport twofold and reduced insulin-stimulated uptake to 62% of the control transport rate dose-dependently, closely correlating with the activation of AMPK. AICAR also inhibited insulin-stimulated GLUT4 translocation, assessed using the plasma membrane lawn assay. The effects of AICAR on insulin-stimulated glucose transport are not mediated by either adenosine receptors or nitric oxide synthase and are mediated downstream of phosphatidylinositol 3′-kinase stimulation. We propose that in contrast to skeletal muscle, in which AMPK stimulation promotes glucose transport to provide ATP as a fuel, AMPK stimulation inhibits insulin-stimulated glucose transport in adipocytes, inhibiting triacylglycerol synthesis, to conserve ATP under conditions of cellular stress. Investigation of the mode of action of AICAR and AMPK may, therefore, give insight into the mechanism of insulin action. *Diabetes* 49: 1649–1656, 2000

Insulin increases glucose transport activity in muscle and fat cells through the translocation of glucose transporter proteins (primarily GLUT4) from an intracellular location to the plasma membrane. The additional glucose uptake stimulated by insulin is used primarily for the synthesis of glycogen and fatty acids in skeletal muscle and adipocytes, respectively. The intracellular insulin signaling pathways that lead to GLUT4 translocation have been extensively investigated, yet only the activation of p85/p110 phosphatidylinositol 3-kinase (PI3K) has been identified as an absolute requirement (1). The participation of the PI3K effector Akt /protein kinase B (PKB) is still being debated (2,3).

A number of other conditions modulate glucose transport in both muscle and adipose tissue. In muscle, exercise is an important stimulus for glucose transport, resulting in increased translocation of GLUT4 at the plasma membrane from intracellular stores (4). In contrast to insulin-stimulated glucose transport, increased glucose transport in response to exercise is used as a source of ATP for the working muscles. Hypoxia and chemical stresses, such as arsenite and azide, have been demonstrated to increase glucose transport in a number of tissues, including adipocytes (5,6). Additionally, treatments that deplete ATP, such as heat shock in hepatocytes (7), exercise in skeletal muscle (8,9), ischemia in heart (10), and glucose deprivation in pancreatic β-cells (11), activate 5′-AMP–activated protein kinase (AMPK). AMPK is the downstream component of a protein kinase cascade activated by a rise in the cellular AMP:ATP ratio and is thought to act as the "fuel gauge" of the mammalian cell (12,13). AMPK can also be artificially activated in intact cells by treatment with 5′-aminoimidazole-4-carboxamide ribonucleoside (AICAR) (14,15). This nucleoside is taken up and accumulates inside the cell as the monophosphorylated nucleotide 5′-aminoimidazole-4-carboxamide ribonucleotide (ZMP), which activates AMPK without disturbing cellular adenine nucleotide ratios (14,15), such that any effects observed are not merely due to depletion of ATP.

Recent studies using AICAR have proposed that AMPK is a mediator of glucose transport in skeletal muscle (16,17). Both contraction and AICAR increase AMPK activity, and the AICAR-stimulated increase in muscle glucose transport is wortmannin insensitive, which suggests that it uses a distinct signaling pathway from insulin (16). Additionally, AICAR has been demonstrated to increase GLUT4 translocation in both skeletal (18) and heart muscle (19). A recent study demonstrated that long-term incubation with AICAR results in increased rat muscle total glycogen, total GLUT4, and hexokinase activity, mimicking the effects of endurance exercise training (20). These studies suggest that the AMPK cascade may be a mediator of exercise-stimulated glucose transport. Because many of the metabolic pathways modulated by insulin also appear to be influenced by AMPK, it has been proposed that perturbation of the AMPK signaling pathway might account for many of the metabolic abnormalities observed in type 2 diabetes (21).

From the Division of Biochemistry and Molecular Biology (I.P.S., G.W.G.), Davidson Building, University of Glasgow; and the University Department of Medicine and Therapeutics (J.M.C.C.), Western Infirmary, Glasgow, U.K.

Address correspondence and reprint requests to Gwyn W. Gould, PhD, Division of Biochemistry and Molecular Biology, Davidson Building, University of Glasgow, Glasgow G12 8QQ, U.K. E-mail: g.gould@bio.gla.ac.uk.

Received for publication 21 March 2000 and accepted in revised form 30 June 2000.

AICAR, 5′-aminoimidazole-4-carboxamide ribonucleoside; AMPK, 5′-AMP–activated protein kinase; DPCPX, 1,3-dipropyl-8-cyclopentylxanthine; DTT, dithiothreitol; eNOS, endothelial nitric oxide synthase; IRAP, insulin-regulated aminopeptidase; IRS, insulin receptor substrate; L-NMMA, N^G-monomethyl-L-arginine; PEG, polyethylene glycol 6000; PI3K, phosphatidylinositol 3-kinase; PKB, protein kinase B; ZMP, 5′-aminoimidazole-4-carboxamide ribonucleotide.

Previous studies in rat epididymal adipocytes have demonstrated AICAR-sensitive AMPK activity (14,22). Incubation of adipocytes with AICAR results in inhibition of isoprenaline-induced lipolysis, mediated in part by direct phosphorylation of hormone-sensitive lipase (14), but the effects of AICAR on adipocyte glucose transport have not been investigated. However, treatment of adipocytes with a number of stimuli, including sorbitol and arsenite, has also been demonstrated to stimulate both AMPK activity (22) and glucose transport (23,24).

In this study, we investigated the role of the AMPK cascade in adipocyte glucose transport, using the 3T3-L1 adipocyte cell line. We report that short-term incubation of cells with AICAR inhibits insulin-stimulated glucose transport, partly due to a reduction in translocation of GLUT4 to the plasma membrane from intracellular stores, which markedly contrasts with previously published data in rat skeletal and cardiac muscle. We provide evidence that the effects of AICAR are unlikely to be mediated by A1 adenosine receptors or by downregulation of the early steps of the insulin signaling pathway. Inhibition of the AMPK substrate endothelial nitric oxide synthase (eNOS), implicated in skeletal muscle exercise-stimulated glucose transport (25), inhibits AICAR-stimulated transport but does not alter AICAR-mediated inhibition of insulin-stimulated glucose transport. These data suggest that the AMPK cascade may be an important mediator of glucose transport in 3T3-L1 adipocytes, which may provide novel therapeutic targets for the treatment of insulin sensitivity in type 2 diabetes.

RESEARCH DESIGN AND METHODS

Materials. AICAR, soybean trypsin inhibitor, 1,3-dipropyl-8-cyclopentylxanthine (DPCPX), and rabbit anti-eNOS antibody were supplied by Sigma (Poole, Dorset, U.K.). [γ-^{32}P]ATP and horseradish peroxidase–conjugated secondary antibodies were from Amersham International (Bucks, U.K.). N^G-monomethyl-L-arginine (L-NMMA) was from Alexis (San Diego, CA). Insulin was from Novo-Nordisk (Copenhagen, Denmark). Type I collagenase was from Worthington (Lakewood, NJ). Rabbit anti-PI3K p85 subunit, sheep anti-PKB pleckstrin homology domain, rabbit anti–insulin receptor substrate-1 (anti-IRS-1), and rabbit anti-IRS-2 antibodies were from Upstate Biotechnology (Lake Placid, NY). Mouse anti-phosphotyrosine antibody was from Santa Cruz Biotechnology (Santa Cruz, CA). Mouse anti–insulin-regulated aminopeptidase (anti-IRAP) was supplied by Drs. L. Garza and M. Birnbaum, University of Pennsylvania. Rabbit anti-GLUT1 was a gift from Dr. S. Baldwin, University of Leeds, U.K. The anti-GLUT4 antibody used was as described previously (26). AMARA peptide (AMARAASAAALARRR) and anti-AMPK α1 and α2 catalytic subunit isoform-specific antibodies have been described elsewhere (27) and were a gift from Prof. D. G. Hardie, University of Dundee, U.K. PKB substrate peptide (RPRAATF) was supplied by Dr. R. Plevin, University of Strathclyde, U. K. All other reagents were from sources described previously (26,28,29).

Cell culture. 3T3-L1 fibroblasts were grown and differentiated as described previously (30). Cells were used 8- to 12-days after differentiation and between passages 4 and 12. Before use, cell monolayers were incubated in serum-free Dulbecco's modified Eagle's medium for 2 h.

Preparation of 3T3-L1 adipocyte lysates and polyethylene glycol 6000 extracts. Cells grown in 100-mm diameter cell culture dishes were preincubated for 1 h at 37°C in 5 ml Krebs-Ringer HEPES buffer (119 mmol/l NaCl, 20 mmol/l Na HEPES, pH 7.4, 5 mmol/l $NaHCO_3$, 4.7 mmol/l KCl, 1.3 mmol/l $CaCl_2$, 1.2 mmol/l $MgSO_4$, 0.1% [wt/vol] bovine serum albumin). The medium was replaced with 5 ml Krebs-Ringer HEPES buffer containing test substances and incubated for various durations at 37°C. The medium was removed, and 0.5 ml lysis/immunoprecipitation buffer (50 mmol/l Tris-HCl pH 7.4 at 4°C, 150 mmol/l NaCl, 50 mmol/l NaF, 5 mmol/l Na pyrophosphate, 2 mmol/l Na orthovanadate, 1 mmol/l EDTA, 1 mmol/l EGTA, 1 mmol/l dithiothreitol [DTT], 0.1 mmol/l benzamidine, 0.1 mmol/l phenylmethylsulfonyl fluoride, 5 mg/l soybean trypsin inhibitor, 1% [vol/vol] Triton X-100, 1% [vol/vol] glycerol) was added. The cell extract was scraped off and transferred to a microcentrifuge tube. Extracts were vortex mixed and centrifuged (14,000*g*, 3 min, 4°C). Supernatants were snap-frozen in liquid N_2 and stored at –80°C before use. Sequential polyethylene glycol 6000 (PEG) precipitation was used to prepare 2.5–6.25% PEG precipitates from some lysates, which were snap-frozen in liquid N_2 and stored at –80°C before AMPK assay (31).

Immunoprecipitation and assay of AMPK. AMPK was immunoprecipitated from lysates and assayed using the AMARA substrate peptide (31). An AMARA peptide kinase could also be detected in PEG precipitates resuspended in HEPES-Brij buffer (50 mmol/l HEPES, pH 7.4, 1 mmol/l DTT, 0.02% [vol/vol] Brij-35) as described previously (31). Protein concentration was determined by the method of Bradford (32).

Determination of 2-deoxy-D-glucose uptake. 2-[^{3}H]deoxy-D-glucose transport was measured in 3T3-L1 adipocytes cultured on six-well plates, as described previously (33). Transport was initiated by the addition of 2-[^{3}H]deoxy-D-glucose (final concentration 50 µmol/l and 1 µCi/ml) to each well. The mixture was then incubated for 3 min. Nonspecific association of radioactivity was determined in parallel incubations in the presence of 10 µmol/l cytochalasin B.

Preparation of epididymal adipocytes and determination of 2-deoxy-D-glucose uptake. Epididymal fat pads were obtained from nonfasted male Wistar rats (Harlan, Bicester, U.K.) killed by CO_2 overdose. Isolated adipocytes were prepared as described previously (34). Adipocytes (10% cytocrit, 950 µl) were incubated at 37°C with shaking in the presence or absence of 1 nmol/l insulin and 500 µmol/l AICAR for 1 h. 2-Deoxy-D-glucose transport was determined using a modification of the method of Ciaraldi and Olefsky (34). Briefly, transport was initiated by adding 50 µl of 0.2 mmol/l 2-[^{3}H]deoxy-D-glucose (specific activity 5,000–10,000 cpm/pmol). After incubation for 3 min at 37°C with shaking, cells were separated by centrifugation through oil and the cell-associated radioactivity assessed by scintillation counting. Nonspecific association of radioactivity was determined in parallel incubations in the presence of 10 µmol/l cytochalasin B.

Plasma membrane lawn assays for GLUT translocation. After experimental manipulations, coverslips of 3T3-L1 adipocytes were rapidly washed in ice-cold buffer for the preparation of plasma membrane lawns, as described previously (28). After fixation, plasma membrane lawns were incubated with anti-GLUT1, anti-GLUT4, or anti-IRAP antibodies followed by incubation with fluorescein isothiocyanate–conjugated secondary antibody. Triplicate coverslips were prepared for each experimental condition. Twelve random images of plasma membrane lawns were collected from each, as described previously (28), and quantified using MetaMorph software (Universal Imaging, West Chester, PA).

Immunoprecipitation of IRS-1 and IRS-2. 3T3-L1 adipocyte lysate (200 µg) was added to 40 µl 25% (vol/vol) Protein A-Sepharose prebound to 2.5 µg rabbit anti-IRS-1 or anti-IRS-2 antibodies. The volume was made up to 300 µl with lysis buffer and mixed for 2 h at 4°C on a rotating mixer. The mixture was then centrifuged (14,000*g*, 30 s, 4°C). The pellet was washed three times with 1 ml lysis buffer and two times with 1 ml lysis buffer without Triton X-100 at 4°C. Immunoprecipitated protein was separated by SDS-PAGE and transferred to nitrocellulose.

Immunoprecipitation and assay of PKB. 3T3-L1 adipocyte lysate (200 µg) was added to 25 µl 25% (vol/vol) Protein G-Sepharose prebound to 5 µg sheep anti-PKB antibody. The volume was made up to 300 µl with lysis buffer and mixed for 2 h at 4°C on a rotating mixer. The mixture was then centrifuged (14,000*g*, 30 s, 4°C), and the pellet was washed three times with 1 ml lysis buffer supplemented with 1 mol/l NaCl and two times with 1 ml HEPES-DTT (50 mmol/l HEPES, pH 7.4, 1 mmol/l DTT) at 4°C. Pellets were resuspended in 30 µl HEPES-DTT and assayed using the following protocol. Reaction mixtures (40 µl) containing 20 µl of HEPES-DTT, 10 µl of 150 µmol/l RPRAATF substrate peptide in HEPES-DTT buffer, and 10 µl of immunoprecipitate were prepared on ice and the reaction initiated by the addition of 10 µl of [γ-^{32}P]ATP solution (250 µmol/l [γ-^{32}P]ATP with a specific activity in the range of 250,000–500,000 cpm/nmol, 50 mmol/l $MgCl_2$). Blank reactions were prepared by substituting HEPES-DTT buffer for substrate peptide. After incubation with shaking at 30°C for 15 min, 40 µl of the reaction mixture was removed and spotted onto 1.5 cm^2 pieces of Whatman P-81 phosphocellulose paper and the paper dropped into 1% (vol/vol) phosphoric acid. The P-81 paper squares were washed for 15 min through three changes of phosphoric acid and then rinsed with water. Rinsed squares were air dried, and the incorporation of ^{32}P into the substrate peptide was determined by Cerenkov radiation in a scintillation counter.

Electrophoresis and immunoblotting. Proteins were electrophoresed on 10 or 15% SDS polyacrylamide gels and transblotted onto nitrocellulose membranes, as described previously (29). Immunolabeled proteins were visualized using horseradish peroxidase–conjugated secondary antibody and the enhanced chemiluminescence system (Amersham).

Statistical analysis. Unless stated otherwise, results are expressed as means ± SE. Statistically significant differences were determined using an independent-samples Student's *t* test.

RESULTS

The expression of two distinct isoforms of the catalytic α-subunit of AMPK (termed α1 and α2) has been demonstrated

in a number of tissues (35,36). Probing of 3T3-L1 adipocyte lysates with either isoform-specific anti-AMPK antibody yielded a 63 kDa band corresponding to each α-subunit isoform (Fig. 1).

Treatment of 3T3-L1 adipocytes with the cell-permeable adenosine analog AICAR elicited a rapid sustained activation of AMPK. The effect could be demonstrated after 5 min and reached a maximum 1.5-fold activation after 30 min (Fig. 2*A*). Activation of AMPK by AICAR was not altered by concurrent incubation with 10 nmol/l insulin (data not shown). The activation of AMPK by AICAR was dose dependent (Fig. 2*B*), such that AMPK was stimulated maximally by 500 µmol/l AICAR, a concentration at which all further experiments were performed. AMPK was assayed in immunoprecipitates of lysates prepared from cells incubated in the presence or absence of AICAR for 60 min. Table 1 illustrates that AMPK complexes containing either the α1 or α2 catalytic subunit isoforms are activated (1.5- and 2.5-fold, respectively) by treatment of the cells with AICAR.

Figure 3 shows the concentration dependence of the effect of AICAR on the uptake of 2-[^{3}H]deoxy-D-glucose into 3T3-L1 adipocytes in the presence or absence of 10 nmol/l insulin. Treatment with insulin alone for 1 h resulted in an increase in glucose uptake of >12-fold. Concomitant incubation with a range of concentrations of AICAR-reduced insulin-stimulated glucose uptake in a dose-dependent fashion (Fig. 3). Maximal inhibition was evident in the presence of 500 µmol/l AICAR, reducing insulin-stimulated glucose uptake to 62% (62.0 ± 11.8, $n = 3$, $P < 0.01$) of the control transport rate. Incubation of rat epididymal adipocytes with 500 µmol/l AICAR resulted in a similar inhibition of insulin-stimulated glucose uptake (data not shown). Figure 3 also shows that over the same range of concentrations, AICAR alone caused a modest twofold (1.8 ± 0.1, $n = 3$, $P < 0.05$) stimulation in basal glucose uptake, also maximal at 500 µmol/l AICAR. The effects of AICAR on basal and insulin-stimulated glucose transport could be observed after incubation for 30 min and were maximal after 60 min (data not shown). Additionally, glucose transport in 3T3-L1 adipocytes incubated for 60 min was inhibited to a similar degree by the addition of AICAR 15 min before or after the addition of insulin (data not shown).

To determine what effect AICAR has on basal and insulin-stimulated GLUT recruitment, we assessed plasma membrane–associated GLUT1, GLUT4, and IRAP using the plasma membrane lawn assay. Insulin-stimulated GLUT4 translocation 4.8 ± 0.4-fold, and this was reduced to 2.5 ± 0.3-fold in the

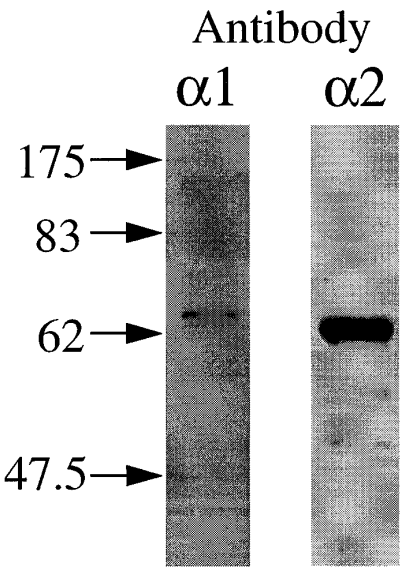

FIG. 1. AMPK-α1 and AMPK-α2 are expressed in 3T3-L1 adipocyte lysates. 3T3-L1 adipocyte lysate proteins were separated by SDS-PAGE, transferred to nitrocellulose, and probed with either anti-AMPK-α1 or anti-AMPK-α2 catalytic subunit isoform-specific antibodies. Horseradish peroxidase–conjugated donkey anti-sheep IgG was used as a secondary antibody. The positions of the various protein markers (in kDa) are indicated. A representative immunoblot is shown, repeated with similar results on three different samples of lysate.

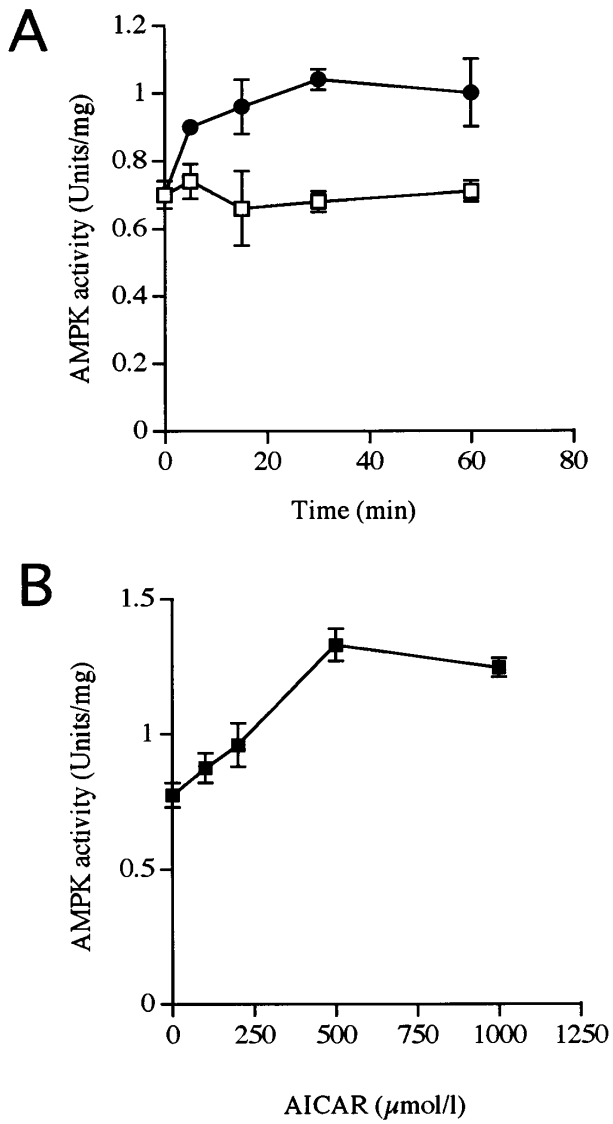

FIG. 2 Characterization of the AMPK activation by AICAR in 3T3-L1 adipocytes. Cells were incubated in the presence (●) or absence (○) of 500 µmol/l AICAR for various times (*A*) or in medium containing various AICAR concentrations for 30 min (*B*). PEG precipitates were prepared and assayed for AMPK activity. The results are expressed as AMPK activity for two separate experiments performed in triplicate. One unit of AMPK activity is that required to incorporate 1 nmol of ^{32}P into the AMARA substrate peptide/min.

TABLE 1
The effect of 500 µmol/l AICAR on catalytic α-subunit isoform-specific AMPK activity in 3T3-L1 adipocytes

Immunoprecipitating antibody	Vehicle control	AICAR 500 µmol/l
AMPK-α1	0.53 ± 0.06	0.79 ± 0.05
AMPK-α2	0.15 ± 0.03	0.38 ± 0.04
AMPK-α1 and AMPK-α2	0.70 ± 0.08	1.15 ± 0.06
Total AMPK activity	0.75 ± 0.17	1.21 ± 0.18

Data are expressed as AMPK activity (units per milligram protein) for two separate experiments performed in triplicate. Lysates (100 µg) prepared from cells incubated for 60 min in the presence or absence of 500 µmol/l AICAR were immunoprecipitated using anti–AMPK-α1, anti–AMPK-α2, or both. The immunoprecipitates were subsequently assayed for AMPK activity. Total AMPK activity was ascertained in PEG precipitates prepared from the same lysates used for immunoprecipitation. One unit of AMPK activity is required to incorporate 1 nmol of ^{32}P into the AMARA substrate peptide per minute.

presence of 500 µmol/l AICAR (n = 3, P < 0.001, Fig. 4). Insulin-stimulated IRAP translocation 4.5 ± 0.3-fold, and this was similarly reduced to 2.8 ± 0.2-fold in the presence of 500 µmol/l AICAR (n = 3, P < 0.001). Neither insulin nor AICAR had any significant effect on GLUT1 translocation.

3T3-L1 adipocytes express adenosine receptors, primarily of the A1 subtype (37). Because AICAR is an adenosine analog, we therefore determined whether the effects of AICAR on glucose transport were mediated by adenosine receptors. Incubation of 3T3-L1 adipocytes with 1 µmol/l DPCPX, an antagonist of adenosine A1 receptors, did not affect basal or insulin-stimulated 2-deoxy-D-glucose uptake or any changes mediated by AICAR (Table 2).

Nitric oxide has been postulated to be a mediator of exercise-stimulated glucose transport in muscle (25). AMPK has recently been demonstrated to phosphorylate and activate eNOS (38). We therefore investigated whether the effects of AICAR on glucose transport were mediated by nitric oxide. Incubation of 3T3-L1 adipocytes with 200 µmol/l L-NMMA, an inhibitor of NOS, inhibited both basal and AICAR-stimulated transport (Table 3) from 1.46 ± 0.10-fold (P < 0.05) to 1.20 ± 0.18-fold (no significant increase) in the presence of L-NMMA. However, L-NMMA did not affect insulin-stimulated 2-deoxy-D-glucose uptake or AICAR-mediated inhibition.

To determine whether the AICAR-mediated inhibition of insulin-stimulated glucose transport is due to inhibition of any of the proximal steps of insulin signaling, we studied basal and insulin-stimulated IRS-1/IRS-2 tyrosine phosphorylation and PI3K recruitment in the presence and absence of 500 µmol/l AICAR. Figure 5 illustrates that insulin substantially stimulated IRS-1 tyrosine phosphorylation and PI3K association compared with control cells. AICAR had no effect on basal or insulin-stimulated conditions on either IRS-1 tyrosine phosphorylation or PI3K association. Neither insulin nor AICAR had a significant effect on IRS-2 tyrosine phosphorylation or PI3K association (data not shown). Additionally, 500 µmol/l AICAR had no effect on basal or insulin-stimulated PKB activity (Fig. 6).

DISCUSSION

Recent studies have demonstrated that exercise and incubation with AICAR stimulates AMPK activity and glucose

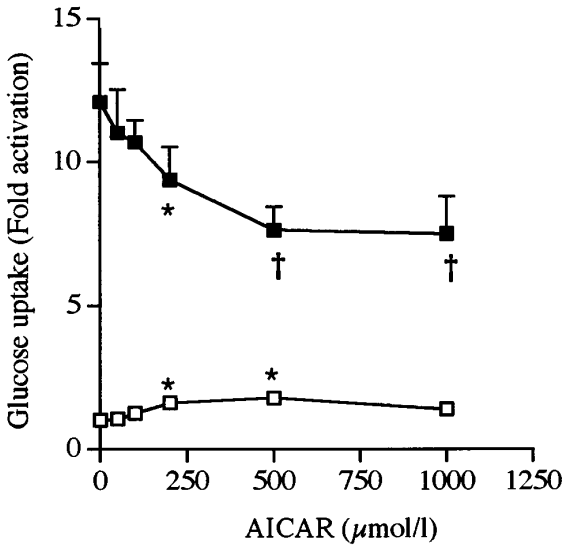

FIG. 3. Effect of extracellular AICAR concentration on basal and insulin-stimulated 2-deoxy-D-glucose uptake. Cells were incubated for 1 h in the presence or absence of 10 nmol/l insulin and a range of AICAR concentrations. The uptake of 2-[^{3}H]deoxy-D-glucose was assayed. The results are expressed as the fold activation relative to basal uptake from three experiments performed in triplicate. *P < 0.05 relative to value in absence of AICAR; †P < 0.01 relative to value in absence of AICAR. Basal glucose uptake was 19 ± 4.0 pmol transported · min^{-1} · mg protein^{-1}.

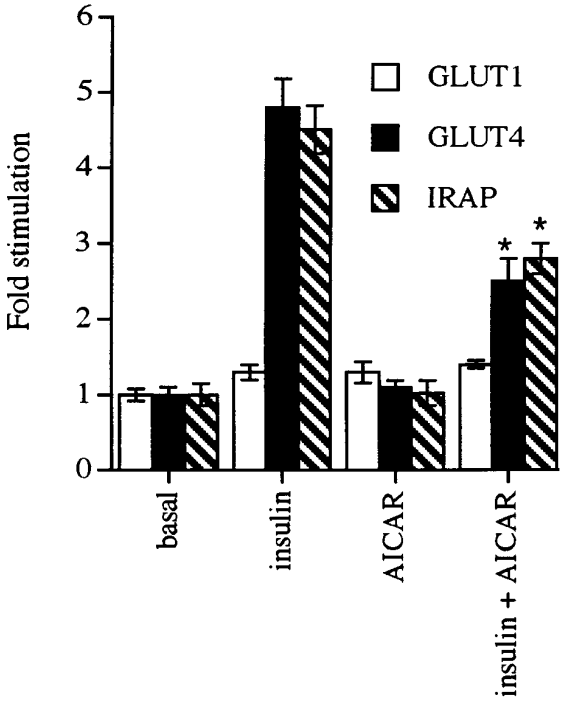

FIG. 4. The effect of 500 µmol/l AICAR on GLUT and IRAP translocation to the plasma membrane. Cells were incubated for 1 h in the presence or absence of 10 nmol/l insulin and 500 µmol/l AICAR, and plasma membrane lawns were prepared. The results are expressed as the fold stimulation in intensity relative to basal from 36 separate images collected from triplicate coverslips stained for GLUT1, GLUT4, and IRAP as indicated. *P < 0.001 relative to value in absence of AICAR.

TABLE 2
The effect of 1 μmol/l DPCPX on glucose transport in 3T3-L1 adipocytes

Treatment	Vehicle control	DPCPX 1 μmol/l
Basal	1.00 ± 0.02	1.09 ± 0.08
Insulin	8.83 ± 0.34	9.05 ± 0.61
AICAR	1.61 ± 0.17	1.56 ± 0.05
Insulin + AICAR	5.73 ± 0.13	5.59 ± 0.45

Data are expressed as the fold activation relative to basal uptake from two experiments performed in triplicate. Cells were incubated for 60 min in the presence or absence of 10 nmol/l insulin, 500 μmol/l AICAR, and 1 μmol/l DPCPX. The uptake of 2-[^{3}H]deoxy-D-glucose was then assayed. Basal transport was 23 ± 0.5 pmol · min^{-1} · mg protein^{-1}.

transport in a wortmannin-insensitive fashion in skeletal muscle (16). This has led to the proposal that the AMPK cascade is an important component of the exercise-stimulated glucose transport signaling pathway. The most significant findings of this study were that AICAR treatment of differentiated 3T3-L1 adipocytes results in an inhibition of insulin-stimulated glucose transport, implying that AMPK has opposing effects in fat and muscle.

It should be noted that ZMP, the intracellular product of AICAR treatment, is not a completely specific activator of AMPK in that it also mimics the effects of AMP on glycogen phosphorylase (39) and fructose-1,6-bisphosphatase (40). However, these effects are unlikely to be of any importance in the regulation of glucose transport in adipocytes, which do not undergo significant gluconeogenesis.

The time and dose dependence of AICAR stimulation of AMPK activity in 3T3-L1 adipocytes (Fig. 2) is similar to other cell lines previously investigated (41–43). Although AMPK activity has been demonstrated previously in adipocytes (14,22), this is the first report, to our knowledge, to demonstrate AMPK expression immunologically in adipocytes or an adipocyte cell line (Fig. 1). Exercise has been reported to stimulate only AMPK complexes containing the α2 subunit isoform in skeletal muscle (44). Table 1 illustrates that the majority of the AMPK activity in 3T3-L1 adipocytes is contributed by the α1 isoform, and AMPK complexes containing either the α1 and α2 catalytic subunit isoforms are activated by AICAR, ~1.5- or 2.5-fold, respectively, compared with basal (Table 1). Because AMPK is assayed in saturating concentrations of AMP, this reflects activation by phosphorylation by AMPK. These differences in the stimulation of each α-subunit isoform may be due to the previously reported enhanced activation of α2 compared with α1 by AMPK in vitro (45).

TABLE 3
The effect of 200 μmol/l L-NMMA on glucose transport in 3T3-L1 adipocytes

Treatment	Vehicle control	L-NMMA 200 μmol/l
Basal	1.00 ± 0.06	0.60 ± 0.09*
Insulin	9.54 ± 0.42†	8.75 ± 0.68†
AICAR	1.46 ± 0.10†	0.72 ± 0.13*
Insulin + AICAR	6.29 ± 0.32†	6.74 ± 0.74†

Data are expressed as the fold activation relative to basal uptake from two experiments performed in triplicate. Cells were incubated for 60 min in the presence or absence of 10 nmol/l insulin, 500 μmol/l AICAR, and 200 μmol/l L-NMMA. The uptake of 2-[^{3}H]deoxy-D-glucose was then assayed. Basal transport was 29 ± 1.7 pmol · min^{-1} · mg protein^{-1}. *P < 0.05 relative to value in absence of L-NMMA; †P < 0.05 relative to value for basal transport.

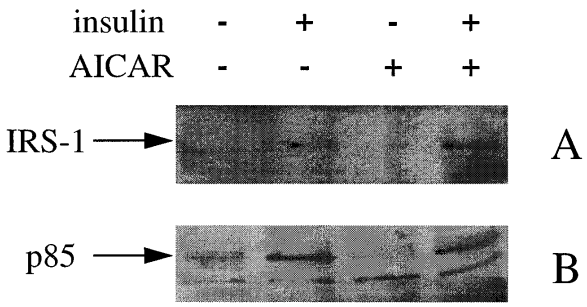

FIG. 5. The effect of 500 μmol/l AICAR on IRS-1 tyrosine phosphorylation and PI3K association. 3T3-L1 adipocytes were incubated in the presence or absence of 500 μmol/l AICAR and 10 nmol/l insulin for 1 h. Lysates were prepared and immunoprecipitated using rabbit anti–IRS-1 antibody. Immunoprecipitates were analyzed by SDS-PAGE, transferred to nitrocellulose, and probed with mouse anti-phosphotyrosine (*A*) or rabbit anti-PI3K p85 subunit antibodies (*B*). Horseradish peroxidase–conjugated secondary antibody was used. Representative immunoblots are shown, repeated with similar results on two different samples of lysates.

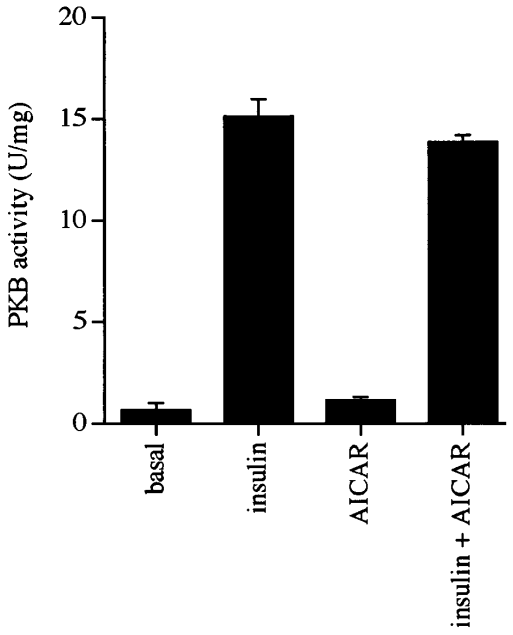

FIG. 6. The effect of 500 μmol/l AICAR on PKB activity in 3T3-L1 adipocytes. Cells were incubated in medium containing 500 μmol/l AICAR and/or 10 nmol/l insulin for 1 h. Lysates were prepared and assayed for PKB activity. The results are expressed as the mean of two separate experiments performed in duplicate. One unit of PKB activity is required to incorporate 1 pmol of ^{32}P into the substrate peptide per minute.

Insulin has been reported to inhibit AMPK activity in isolated hepatocytes (46) and heart (47). Insulin treatment does not appear, however, to alter AMPK activity in the liver-derived H4IIE cell line (42). In agreement with the latter study, incubation of 3T3-L1 adipocytes with 10 nmol/l insulin did not alter AMPK activity.

Figure 3 illustrates that incubation of 3T3-L1 adipocytes with 500 μmol/l AICAR for 1 h modestly stimulates basal glucose transport 1.8-fold, but dramatically reduces insulin-stimulated transport to 62% of the transport rate in the presence of insulin alone. The incubation time required for the effects of AICAR to be observed on glucose transport does not precede the stimulation of AMPK, and the dose dependence of AICAR-mediated inhibition of insulin-stimulated glucose transport also correlates with the dose dependence of AMPK activation. These data support the hypothesis that the effects of AICAR are mediated by AMPK. Treatment with glucosamine and oxidative stress have also been demonstrated to inhibit insulin-stimulated glucose transport in 3T3-L1 adipocytes (48,49). It is possible that the effects of glucosamine are AMPK-mediated, as this treatment depletes cellular ATP (48). In contrast, oxidative stress–mediated inhibition of insulin-stimulated transport appears to be mediated by the inhibition of insulin receptor and IRS-1 tyrosine phosphorylation (49). A recent study illustrated decreased glucose uptake and oxidation in human endothelial cells incubated for 2 h in 2 mmol/l AICAR (41). This inhibition of basal glucose uptake may reflect yet another mechanism by which AMPK modulates glucose metabolism in certain cell types. However, incubation with AICAR for 2 h may affect transcription and expression of genes involved in carbohydrate and fat metabolism to influence glucose uptake and oxidation (42,50,51), whereas the more acute time course used in this study is unlikely to affect gene expression.

Adenosine receptor activation was demonstrated to augment insulin-stimulated glucose transport in adipocytes (52,53). Concurrent incubation of cells with the A1 adenosine receptor antagonist DPCPX did not influence basal or insulin-stimulated glucose transport or the effects of AICAR. It seems unlikely, therefore, that the effects of AICAR, which is an adenosine analog, are mediated by A1 adenosine receptors, either as an agonist or antagonist. Previous studies of glucose transport in skeletal and heart muscle also demonstrated that the effects of AICAR are not mediated by adenosine receptors (17,19).

AICAR and nitric oxide donors have similar effects on skeletal muscle glucose transport (16,25). Both AMPK (38) and PKB (54,55) have been reported to phosphorylate and activate eNOS at a common site. Adipocytes (56) and 3T3-L1 adipocytes (I.P.S. and G.W.G., unpublished observations) also express eNOS, such that activation of AMPK may result in the stimulation of nitric oxide production. Incubation of cells with the eNOS inhibitor L-NMMA inhibited the modest stimulation of basal transport by AICAR, suggesting that this may be mediated by AMPK-mediated activation of eNOS. PKB stimulation by insulin would be expected to have similar effects, because it phosphorylates and activates eNOS at the same site (38,54,55). However, incubation with L-NMMA did not influence insulin-stimulated transport in the presence or absence of AICAR, precluding nitric oxide as a mediator of insulin-stimulated glucose transport or the inhibition of insulin-stimulated transport by AICAR.

The profound inhibition of insulin-stimulated GLUT4 and IRAP translocation to the plasma membrane by AICAR (Fig. 4) suggests that AICAR-mediated inhibition of insulin-stimulated glucose transport is, at least in part, due to either reduced recruitment of GLUT4 to the plasma membrane or a consequence of inhibition of GLUT4 vesicle fusion at the plasma membrane. The trafficking of IRAP has been demonstrated to be identical to that of GLUT4 (57). Accordingly, insulin-stimulated IRAP translocation was inhibited to a degree similar to that of GLUT4 (Fig. 4). The modest stimulation of basal glucose uptake by AICAR may also be mediated by increased GLUT1/GLUT4 translocation to the plasma membrane, but the effect is likely to be too small to be detected using the plasma membrane lawn assay.

Incubation with AICAR has no effect on basal or insulin-stimulated IRS-1 tyrosine phosphorylation or PI3K recruitment (Fig. 5). This suggests that the effects of AICAR on insulin-stimulated glucose transport and GLUT4 translocation are mediated downstream of PI3K stimulation. Neither insulin nor AICAR alter IRS-2 tyrosine phosphorylation or PI3K association. IRS-2 tyrosine phosphorylation and PI3K association have been reported to be attenuated compared with IRS-1 and occur more transiently than the 1-h incubation time used in this study (58). In adipocytes, insulin has been reported to specifically activate PKB-β (59). It is, however, a matter of debate, despite intensive investigation, whether PKB stimulation is an absolute requirement for insulin-stimulated glucose transport (2,3). The fact that AICAR does not alter basal or insulin-stimulated PKB activation (Fig. 6) is further evidence that the initial steps of insulin signaling are unaffected by AMPK stimulation. Phosphorylation of IRS-1 on serine and threonine residues has been reported to attenuate insulin signaling and glucose transport in 3T3-L1 adipocytes (60). Candidate IRS-1 kinases have included glycogen synthase kinase-3 (61), protein kinase C (62), and mitogen-activated protein kinase (63). The data presented in this study cannot preclude AICAR/AMPK-mediated serine/threonine phosphorylation of IRS-1/2, which might well have more subtle effects on insulin signaling than those reported in this study.

Isoprenaline has been demonstrated to activate AMPK in rat epididymal adipocytes (22). During exercise, a proportion of the increase in adipocyte lipolysis is considered to be mediated by the stimulation of adipocyte β-adrenoreceptors (64). During prolonged exercise, therefore, AMPK may also become activated in adipocytes to prevent the ATP-consuming futile cycle of fatty acid reesterification that occurs when the rate of fatty acid export does not match the rate of lipolysis (12), inhibiting both surplus lipolysis and any insulin-stimulated glucose transport.

In skeletal muscle, AICAR has been demonstrated to translocate GLUT4 to the plasma membrane (18). This AMPK-mediated pathway is distinct from that activated by insulin (16) and may link the supply of fuel, in the form of glucose, to the energy requirements of muscle during exercise (21). In adipocytes, the insulin-stimulated increase in cytoplasmic glucose is used anabolically to produce fatty acids and triacylglycerol for export to other tissues. Under the conditions of cellular stress by which AMPK is activated, it seems prudent that adipocyte insulin-stimulated glucose transport is inhibited, to conserve the ATP used in fatty acid and triacylglycerol synthesis. The fact that AICAR-stimulated AMPK activation has different effects on fat and muscle glucose transport implies

that the mode of action of AICAR/AMPK in each tissue must involve either distinct signaling pathways or alternative modulation of the same pathway. Similarly, the effects of AICAR in muscle and fat appear to be independent of the early steps of the insulin signaling pathway.

ACKNOWLEDGMENTS

This work was supported by the University of Glasgow, the Medical Research Council (cooperative group grant to J.M.C.C. and G.W.G.), and Tenovus (Scotland) (G.W.G.).

REFERENCES

1. Heller-Harrison RA, Morin M, Guilherme A, Czech MP: Insulin-mediated targeting of phosphatidylinositol 3-kinase to GLUT4-containing vesicles. *J Biol Chem* 271:10200–10204, 1996
2. Calera MR, Martinez C, Liu H, El Jack AK, Birnbaum MJ, Pilch PF: Insulin increases the association of Akt-2 with Glut4-containing vesicles. *J Biol Chem* 273:7201–7204, 1998
3. Kitamura T, Ogawa W, Sakaue H, Hino Y, Kuroda S, Takata M, Matsumoto M, Maeda T, Konishi H, Kikkawa U, Kasuga M: Requirement for activation of the serine-threonine kinase Akt (protein kinase B) in insulin stimulation of protein synthesis but not of glucose transport. *Mol Cell Biol* 18:3708–3717, 1998
4. Hayashi T, Wojtaszewski JFP, Goodyear LJ: Exercise regulation of glucose transport in skeletal muscle. *Am J Physiol* 273:E1039–E1051, 1997
5. Barros LF, Marchant RB, Baldwin SA: Dissection of stress-activated glucose transport from insulin-induced glucose transport in mammalian cells using wortmannin and ML-9. *Biochem J* 309:731–736, 1995
6. Zhang J-Z, Behrooz A, Ismail-Beigi F: Regulation of glucose transport by hypoxia. *Am J Kidney Dis* 34:189–202, 1999
7. Corton JM, Gillespie JG, Hardie DG: Role of the AMP-activated protein kinase in the cellular stress response. *Curr Biol* 4:315–324, 1994
8. Winder WW, Hardie DG: Inactivation of acetyl-CoA carboxylase and activation of AMP-activated protein kinase in muscle during exercise. *Am J Physiol* 270:E299–E304, 1996
9. Hutber CA, Hardie DG, Winder WW: Electrical stimulation inactivates muscle acetyl-CoA carboxylase and increases AMP-activated protein kinase. *Am J Physiol* 272:E262–E266, 1997
10. Kudo N, Barr AJ, Barr RL, Desai S, Lopaschuk GD: High rates of fatty acid oxidation during reperfusion of ischemic hearts are associated with a decrease in malonyl-CoA levels due to an increase in 5′-AMP-activated protein kinase inhibition of acetyl-CoA carboxylase. *J Biol Chem* 270:17513–17520, 1995
11. Salt IP, Johnson G, Ashcroft SJH, Hardie DG: AMP-activated protein kinase is activated by low glucose in cell lines derived from pancreatic β cells, and may regulate insulin release. *Biochem J* 335:533–539, 1998
12. Hardie DG, Carling D: The AMP-activated protein kinase: fuel gauge of the mammalian cell? *Eur J Biochem* 246:259–273, 1997
13. Hardie DG, Carling D, Carlson M: The AMP-activated/SNF1 protein kinase subfamily: metabolic sensors of the eukaryotic cell? *Annu Rev Biochem* 67:821–855, 1998
14. Corton JM, Gillespie JG, Hawley SA, Hardie DG: 5-aminoimidazole-4-carboxamide ribonucleoside: a specific method for activating AMP-activated protein kinase in intact cells? *Eur J Biochem* 229:558–565, 1995
15. Henin N, Vincent MF, Gruber HE, Van den Berghe G: Inhibition of fatty acid and cholesterol synthesis by stimulation of AMP-activated protein kinase. *FASEB J* 9:541–546, 1995
16. Hayashi T, Hirshman MF, Kurth EJ, Winder WW, Goodyear LJ: Evidence for 5′ AMP-activated protein kinase mediation of the effect of muscle contraction on glucose transport. *Diabetes* 47:1369–1373, 1998
17. Bergeron R, Russell RR, Young LH, Ren J-M, Marcucci M, Lee A, Schulman GI: Effect of AMPK activation on muscle glucose metabolism in conscious rats. *Am J Physiol* 276:E938–E944, 1999
18. Kurth-Kraczek EJ, Hirshman MF, Goodyear LJ, Winder WW: 5′ AMP-activated protein kinase activation causes GLUT4 translocation in skeletal muscle. *Diabetes* 48:1667–1671, 1999
19. Russell RR, Bergeron R, Shulman GI, Young LH: Translocation of myocardial GLUT-4 and increased glucose uptake through activation of AMPK by AICAR. *Am J Physiol* 277:H643–H649, 1999
20. Holmes BF, Kurth-Kraczek EJ, Winder WW: Chronic activation of 5′-AMP-activated protein kinase increases GLUT-4, hexokinase, and glycogen in muscle. *J Appl Physiol* 87:1990–1995, 1999
21. Winder WW, Hardie DG: AMP-activated protein kinase, a metabolic master switch: possible roles in type 2 diabetes. *Am J Physiol* 277:E1–E10, 1999
22. Moule SK, Denton RM: The activation of p38 MAPK by the β-adrenergic agonist isoproterenol in rat epididymal fat cells. *FEBS Lett* 439:287–290, 1998
23. Chen D, Elmendorf JS, Olson AL, Li X, Earp HS, Pessin JE: Osmotic shock stimulates GLUT4 translocation in 3T3L1 adipocytes by a novel tyrosine kinase pathway. *J Biol Chem* 272:27401–27410, 1997
24. Sviderskaya EV, Jazrawi E, Baldwin SA, Widnell CC, Pasternak CA: Cellular stress causes accumulation of the glucose transporter at the surface of cells independently of their insulin sensitivity. *J Membr Biol* 149:133–140, 1996
25. Roberts CK, Barnard RJ, Scheck SH, Balon TW: Exercise-stimulated glucose transport in skeletal muscle is nitric oxide dependent. *Am J Physiol* 273:E220–E225, 1997
26. Millar CA, Shewan A, Hickson GRX, James DE, Gould GW: Differential regulation of secretory compartments containing the insulin-responsive glucose transporter 4 in 3T3-L1 adipocytes. *Mol Biol Cell* 10:3675–3688, 1999
27. Woods A, Salt I, Scott J, Hardie DG, Carling D: The α1 and α2 isoforms of the AMP-activated protein kinase have similar activities in rat liver but exhibit differences in substrate specificity in vitro. *FEBS Lett* 397:347–351, 1996
28. Martin LB, Shewan A, Millar CA, Gould GW, James DE: Vesicle-associated membrane protein 2 plays a specific role in the insulin-dependent trafficking of the facilitative glucose transporter GLUT4 in 3T3-L1 adipocytes. *J Biol Chem* 273:1444–1452, 1998
29. Gould GW, Brant AM, Kahn BB, Shepherd PR, McCoid SC, Gibbs EM: Expression of the brain-type glucose transporter is restricted to brain and neuronal cells in mice. *Diabetologia* 35:304–309, 1992
30. Frost SC, Lane MD: Evidence for the involvement of vicinal sulfhydryl groups in insulin-activated hexose transport by 3T3-L1 adipocytes. *J Biol Chem* 260:2646–2652, 1985
31. Hardie DG, Haystead TAJ, Salt IP, Davies SP: Assay and purification of protein: serine/threonine kinases. In *Protein Phosphorylation: A Practical Approach*. 2nd ed. Hardie DG, Ed. Oxford, U.K., Oxford University Press, 1999, p. 201–209
32. Bradford MM: A rapid and sensitive method for the quantitation of microgram quantities of protein utilizing the principle of protein-dye binding. *Anal Biochem* 72:248–254, 1976
33. Gibbs EM, Lienhard GE, Gould GW: Insulin-induced translocation of glucose transporters to the plasma membrane precedes full stimulation of hexose transport. *Biochemistry* 27:6681–6685, 1988
34. Ciaraldi TP, Olefsky JM: Effect of temperature on coupling of insulin receptors to stimulation of glucose transport in isolated rat adipocytes. *Metabolism* 32:1002–1008, 1983
35. Stapleton D, Mitchelhill KI, Gao G, Widmer J, Michell BJ, Teh T, House CM, Fernandez CS, Cox T, Witters LA, Kemp BE: Mammalian AMP-activated protein kinase subfamily. *J Biol Chem* 271:611–614, 1996
36. Cheung PCF, Salt IP, Davies SP, Hardie DG, Carling D: Characterization of AMP-activated protein kinase γ-subunit isoforms and their role in AMP binding. *Biochem J* 346:659–669, 2000
37. Collis MG, Hourani SMO: Adenosine receptor subtypes. *Trends Pharmacol Sci* 14:360–366, 1993
38. Chen Z-P, Mitchelhill KI, Michell BJ, Stapleton D, Rodriguez-Crespo I, Witters LA, Power DA, Ortiz de Montellano PR, Kemp BE: AMP-activated protein kinase phosphorylation of endothelial NO synthase. *FEBS Lett* 443:285–289, 1999
39. Young ME, Radda GK, Leighton B: Activation of glycogen phosphorylase and glycogenolysis in rat skeletal muscle by AICAR—an activator of AMP-activated protein kinase. *FEBS Lett* 382:43–47, 1996
40. Vincent MF, Marangos P, Gruber HE, Van den Berghe G: AICAriboside inhibits gluconeogenesis in isolated rat hepatocytes. *Adv Exp Med Biol* 309B:359–362, 1991
41. Dagher Z, Ruderman N, Tornheim K, Ido Y: The effect of AMP-activated protein kinase and its activator AICAR on the metabolism of human umbilical vein endothelial cells. *Biochem Biophys Res Comm* 265:112–115, 1999
42. Lochhead PA, Salt IP, Walker KS, Hardie DG, Sutherland C: 5-Aminoimidazole-4-carboxamide riboside mimics the effects of insulin on the expression of the two key gluconeogenic genes, PEPCK and glucose-6-phosphatase. *Diabetes* 49:896–903, 2000
43. Hardie DG, Salt IP, Hawley SA, Davies SP: AMP-activated protein kinase: an ultrasensitive system for monitoring cellular energy charge. *Biochem J* 338:717–722, 1999
44. Vavvas D, Apazidis A, Saha AK, Gamble J, Patel A, Kemp BE, Witters LA, Ruderman NB: Contraction-induced changes in acetyl CoA carboxlase and 5′-AMP-activated kinase in skeletal muscle. *J Biol Chem* 272:13255–13261, 1997
45. Salt I, Celler JW, Hawley SA, Prescott A, Woods A, Carling D, Hardie DG: AMP-activated protein kinase: greater AMP dependence, and preferential nuclear localization, of complexes containing the α2 isoform. *Biochem J* 334:177–187, 1998
46. Witters LA, Kemp BE: Insulin activation of acetyl-CoA carboxylase accom-

panied by inhibition of the 5′-AMP-activated protein kinase. *J Biol Chem* 267:2864–2867, 1992
47. Gamble J, Lopaschuk GD: Insulin inhibition of 5′ adenosine monophosphate-activated protein kinase in the heart results in activation of acetyl coenzyme A carboxylase and inhibition of fatty acid oxidation. *Metabolism* 46:1270–1274, 1997
48. Hresko RC, Heimberg H, Chi MM, Mueckler M: Glucosamine-induced insulin resistance in 3T3-L1 adipocytes is caused by depletion of intracellular ATP. *J Biol Chem* 273:20658–20668, 1998
49. Hansen LL, Ikeda Y, Olsen GS, Busch AK, Mosthaf L: Insulin signaling is inhibited by micromolar concentrations of H_2O_2: evidence for a role of H_2O_2 in tumor necrosis factor alpha-mediated insulin resistance. *J Biol Chem* 274:25078–25084, 1999
50. Leclerc I, Kahn A, Doiron B: The 5′-AMP-activated protein kinase inhibits the transcriptional stimulation by glucose in liver cells, acting through the glucose response complex. *FEBS Lett* 431:180–184, 1998
51. Foretz M, Carling D, Guichard C, Ferre P, Foufelle F: AMP-activated protein kinase inhibits the glucose-activated expression of fatty acid synthase gene in rat hepatocytes. *J Biol Chem* 273:14767–14771, 1998
52. Kuroda M, Honnor RC, Cushman SW, Londos C, Simpson IA: Regulation of insulin-stimulated glucose transport in the isolated rat adipocyte: cAMP-independent effects of lipolytic and antilipolytic agents. *J Biol Chem* 262:245–253, 1987
53. Ferrara CM, Cushman SW: GLUT4 trafficking in insulin-stimulated rat adipose cells: evidence that heterotrimeric GTP-binding proteins regulate the fusion of docked GLUT4-containing vesicles. *Biochem J* 343:571–577, 1999
54. Fulton D, Gratton J-P, McCabe TJ, Fontana J, Fujio Y, Walsh K, Franke TF, Papapetropoulos A, Sessa WC: Regulation of endothelium-derived nitric oxide production by the protein kinase Akt. *Nature* 399:597–601, 1999
55. Dimmeler S, Fleming I, Fisslthaler B, Hermann C, Busse R, Zeiher AM: Activation of nitric oxide synthase in endothelial cells by Akt-dependent phosphorylation. *Nature* 399:601–605, 1999
56. Ribiere C, Jaubert AM, Gaudiot N, Sabourault D, Marcus ML, Boucher JL, Denis-Henriot D, Giudicelli Y: White adipose tissue nitric oxide synthase: a potential source for NO production. *Biochem Biophys Res Commun* 222:706–712, 1996
57. Garza LA, Birnbaum MJ: Insulin-responsive aminopeptidase trafficking in 3T3-L1 adipocytes. *J Biol Chem* 275:2560–2567, 2000
58. Inoue G, Cheatham B, Emkey R, Kahn CR: Dynamics of insulin signaling in 3T3-L1 adipocytes: differential compartmentalization and trafficking of insulin receptor substrate (IRS)-1 and IRS-2. *J Biol Chem* 273:11548–11555, 1998
59. Hill MM, Clark SF, Tucker DF, Birnbaum MJ, James DE, Macaulay SL: A role for protein kinase Bβ/Akt2 in insulin-stimulated GLUT4 translocation in adipocytes. *Mol Cell Biol* 19:7771–7781, 1999
60. Mothe I, Van Obberghen E: Phosphorylation of insulin receptor substrate-1 on multiple serine residues, 612, 632, 662, and 731, modulates insulin action. *J Biol Chem* 271:11222–11227, 1996
61. Eldar-Finkelman H, Krebs EG: Phosphorylation of insulin receptor substrate 1 by glycogen synthase kinase 3 impairs insulin action. *Proc Natl Acad Sci U S A* 94:9660–9664, 1997
62. De Fea K, Roth RA: Protein kinase C modulation of insulin receptor substrate-1 tyrosine phosphorylation requires serine 612. *Biochemistry* 36: 12939–12947, 1997
63. De Fea K, Roth RA: Modulation of insulin receptor substrate-1 tyrosine phosphorylation and function by mitogen-activated protein kinase. *J Biol Chem* 272:31400–31406, 1997
64. Arner P: Impact of exercise on adipose tissue metabolism in humans. *Int J Obesity* 19:S18–S21, 1995